THE DEVELOPMENT OF A 3D MHD CODE IN COMSOL MULTIPHYSICS AND ITS APPLICATION TO MHD FLOW IN A RIPPLED MAGNETIC FIELD

JUN WANG,^{a*} LONG ZHANG,^a QIXIANG CAO,^a FENGCHAO ZHAO,^a and XINGHUA WU,^a Southwestern Institute of Physics Chengdu, China Email: jwang cn@qq.com

Abstract

In fusion liquid metal blankets, the motion of liquid metals within the plasma-confining magnetic field induces magnetic fields/currents and generates Lorentz forces, leading to characteristic velocity profiles and significant pressure drops—a phenomenon known as magnetohydrodynamics (MHD). Numerical simulation is an effective tool for investigating MHD performance. In this study, a 3D MHD numerical code was developed on the COMSOL Multiphysics platform by solving the magnetic induction equation and modified Navier-Stokes equations. The code's validity was rigorously verified against benchmark cases, including analytical solutions for the Shercliff and Hunt configurations, MHD experimental data under non-uniform magnetic fields, and comparisons with a well-validated reference code. Excellent agreement in detailed calculations confirms the high reliability of the developed code, which can simulate fully developed laminar MHD flows under uniform magnetic fields and the transitions from ordinary flow to fully developed MHD flows in gradient magnetic fields. Building on this validation, the code was used to investigate MHD flow behaviour in longitudinally varying background magnetic fields, analysing the mechanisms by which magnetic field gradients affect MHD pressure drops and boundary jet flows. Further, the code was applied to analyse liquid lithium-lead blanket components: the inlet and outlet pipes, which pass through the inter-coil gaps where the magnetic field exhibits significant gradients due to toroidal field rippling. Calculations of pressure drops induced by this rippled magnetic field showed good agreement with the prediction of 2D fully developed MHD pressure drops, indicating that additional 3D MHD pressure drops induced by the gradient magnetic field are negligible in the studied scenarios. This supports the practical utility of 2D approximations for evaluating pressure drops in such blanket pipe designs

1. INTRODUCTION

Liquid metal blankets are among the most promising candidates for fusion blanket technology. The flow of liquid metal in fusion blankets is subject to strong plasma-confining magnetic fields and the magnetic field has a significant effect on its flow profiles and pressure drops. This phenomenon is the so-called liquid metal Magnetohydrodynamics(MHD)^{[1][2]}. The development of a reliable 3D MHD numerical simulation code is of crucial importance to MHD research and blanket design. There are several 3D MHD codes developed for fusion application. Their electromagnetic models generally fall into two categories, one category is developed by applying the magnetic induction formulation, which is characteristic of intrinsic current conservation^[3]. This group includes the HIMAG code^[4]. The other category is by using the electric potential formulation, among which has the MHD-UCAS code^[5]. An additional consistency conservation scheme technique is mandatory in this kind of code to achieve current conservation^[6]. The design of blankets has been facilitated by the utilization of various MHD codes. The MHD-UCAS code pioneered the simulation of thermal MHD flow in a prototypical dual coolant lead lithium (DCLL) blanket module, achieving an impressive Hartmann number 10⁴ and Grashof number 10^{12[7][8]}. The buoyant and pressure-driven fully developed laminar MHD flows in a square duct are validated on ANSYS CFX by applying electrical potential formulation, while the thermal MHD flow in a typical unit of Water-Cooled Lithium Lead (WCLL) blanket is simulated^[9]. Additionally, there are other robust MHD codes that have been reported in the literature without formal naming, thus precluding their inclusion here.

Since MHD codes are not shared within fusion community, this urges many laboratories to develop their own MHD codes to study the liquid metal flow. Commercial software platforms with built-in equation customization features are deemed as a good alternative choice for developing MHD codes. Among those, COMSOL Multiphysics has a mathematical module for equation definition and a wide range of solvers available and it has been commonly proposed as an efficient approach to quickly develop a more user-friendly 3D MHD code for liquid metal blanket application. Although the electric potential formulation has been extensively developed and validated in numerous MHD codes within COMSOL Multiphysics and other commercial software packages [9][10][11], it remains crucial to note that these codes lack a consistent conservation scheme—a limitation that gives rise to additional concerns. Implementing such a scheme in COMSOL Multiphysics requires modifying its source code, posing significant challenges for the users of commercial software. In contrast, this study adopts the magnetic induction equation to develop an MHD code, thereby circumventing the need for consistency conservation schemes. Therefore, the objective of this study is to propose a novel approach for the rapid development of 3D MHD code by incorporating magnetic induction formulas and modified Navier-Stokes equations into COMSOL Multiphysics, while simultaneously demonstrating the robustness of the developed

MHD codes through recommended examples, including analytical solutions for fully developed 3D MHD flows, the ALEX experimental data on MHD flows in rectangular duct under gradient magnetic fields, and results corroborated by other literature. Moreover, the 3D MHD effect in the rectangular duct under a gradient magnetic field is investigated, and the impact of magnetic field gradient on pressure drops and boundary jet is analysed. Furthermore, the above calculation method was applied to the analysis of real blanket components. For the liquid lithium-lead blanket, its inlet and outlet pipes invariably need to pass through the gap between the two coils, where the magnetic field exhibits significant gradient characteristics. For this scenario, the pressure drops induced by this special magnetic field distribution was calculated using the above-verified calculation example.

MATHEMATICAL FORMULATIONS

The liquid metal MHD flow in blankets, under normal operating conditions, involves the steady movement of an incompressible, viscous fluid with high conductivity within a static strong magnetic field. In this context, the magnetic Reynolds number is sufficiently small to justify the use of the inductionless approximation^[1]. The magnetic field can be divided into the applied and induced components, where the induced field is significantly smaller than the applied field (B=B₀+B_i=B₀). Consequently, the contribution of the induced magnetic field to the Lorentz force term in the momentum equation can be neglected. The Lorentz force term is then represented as $J \times B_{\theta}$. This approach is commonly referred to as inductionless approximation. It is important to note that this study exclusively focuses on laminar flow and quasi-steady-state problems, thus rendering the time term in the physical model negligible. Therefore, the governing equations-including the mass conservation equation and the modified Navier-Stokes equation, are given by^[12].

$$\rho \nabla \cdot \mathbf{V} = 0 \tag{1}$$

$$\rho \nabla \cdot \mathbf{V} = 0$$

$$\rho (\mathbf{V} \cdot \nabla) \mathbf{V} = -\nabla P + \mu \nabla^2 \mathbf{V} + \mathbf{J} \times \mathbf{B_0}$$
(1)
(2)

In above equations, V is the velocity, P is the pressure, μ is the dynamic viscosity, ρ is the density, J is the current density and B_0 is the applied magnetic field. Regarding the magnetic induction formulation, as previously stated, the source-free character of the magnetic divergence term allows it to be dropped, simplifying the magnetic induction formulation. This simplified version is often referred to as the B formulation. For simplicity, B refers And the induced magnetic field in solid walls satisfies following equation: $\frac{1}{\eta}\nabla^2 \mathbf{B} = (\mathbf{V}\cdot\nabla)\mathbf{B_0} - (\mathbf{B_0}\cdot\nabla)\mathbf{V}$ And the induced magnetic field in solid walls satisfies following equation: $\frac{1}{\eta}\nabla^2 \mathbf{B} = 0$ Here, $\eta = \mu_0 \sigma$, η is the magnetic diffusion.

$$\frac{1}{\eta} \nabla^2 \mathbf{B} = (\mathbf{V} \cdot \nabla) \mathbf{B_0} - (\mathbf{B_0} \cdot \nabla) \mathbf{V} \tag{3}$$

$$\frac{1}{\eta}\nabla^2 \mathbf{B} = 0\tag{4}$$

Here, $\eta = \mu_0 \sigma$, η is the magnetic diffusion coefficient and μ_0 is vacuum magnetic permeability, σ is the wall or fluid conductivity. Typical boundary conditions for velocity and pressure are Dirichlet, Neumann, or periodic at inlet, outlet, and walls, just like other normal CFD codes. The pseudo-vacuum boundary condition, which is a general convenient approximation of the realistic induced magnetic field B=0 far from the flow domain, is applied to define the induced magnetic field on simulation domain surface^[13].

$$\mathbf{n} \times \mathbf{B} = 0 \tag{5}$$

$$\mathbf{n} \cdot \nabla \mathbf{B} = 0 \tag{6}$$

Where n is the surface normal vector. The B formulation is implemented through a mathematical module in COMSOL Multiphysics. The elimination of the terms on the right-hand side of the equation is specifically applicable to solid wall domains. The B formulation, encompassing both fluid and solid domains, is unified within a single equation framework using identical variables to ensure continuity of tangential magnetic fields and current density at the interface between solids and fluids. This can be expressed as:

$$J = \frac{1}{\mu_0} \nabla \times \mathbf{B} \tag{7}$$

The B equations and modified Navier-Stokes equations are fully coupled using the default settings provided by COMSOL Multiphysics. For solving steady-state problems in this study, an iterative solution approach is adopted based on Newton's method within the COMSOL Multiphysics framework, initializing dependent variables manually. Specifically, we employed in-built MUMPS solver that utilizes LU decomposition technique to handle stiffness matrix computations and derive solutions for dependent variables. Moreover, a convergence criterion of a relative error of 0.001 was defined as termination condition for calculations.

VALIDATION OF 3D FULLY DEVELOPED LAMINAR MHD CASES

Exact analytical solutions for fully developed, incompressible laminar flows in rectangular ducts with a transverse magnetic field are found to exist under specific conditions, such as the Shercliff and Hunt cases^{[14][15]}. The analytical solutions obtained from these two cases will be utilized to validate the code developed in this study. In the context of MHD flow within a straight rectangular duct, the walls perpendicular to the applied magnetic field are referred to as Hartmann walls, while the walls parallel to the magnetic field are known as side walls^[2]. In Shercliff's case, all walls of the rectangular duct are electrically insulated, while in Hunt's case, only the side walls are electrically insulated. The geometric model for these two scenarios is illustrated in Fig. 1, where half-length of the Hartmann wall is denoted as 'a' and the half side wall length is indicated as 'b', with the magnetic field direction set along the x-axis. The non-dimensional parameters employed to characterize the MHD flow encompass the Hartmann number ($\mathbf{H}\mathbf{a} = \mathbf{B_0}b\sqrt{\frac{\sigma_f}{\mu}}$), the wall conduction ratio ($C_w = \frac{t_w\sigma_w}{b\sigma_f}$), and the channel aspect

ratio ($\chi = \frac{b}{a}$), where t_w is the wall thickness, σ_w is the wall conductivity, σ_f is the fluid conductivity. For laminar flow, a no-slip condition (V=0) is imposed at the walls, while a pressure difference is established between the inlet and outlet. Periodic boundary conditions are set on the velocity at both ends. In this study, calculations are conducted for two cases proposed by Shercliff and two cases proposed by Hunt. Table I presents a summary of these four cases along with their corresponding non-dimensional parameters and results. The non-dimensional parameters for Case 1 and Case 3 are consistent with those presented in Reference [16], while the parameters for Case 2 and Case 4 align with those reported in Reference [6]. The comparison between computational results and analytical solutions for all four cases is illustrated in Fig. 2 and Fig. 3, depicting the velocity distribution on the mid-plane (x/b=0). The normalized velocity profile on the cross-section is shown in Fig. 4. In these figures, the x-coordinate and y-coordinate are normalized by the half side wall length, b, and the velocity is normalized by the average velocity, V0. The numerical velocity profiles exhibit excellent agreement with the analytical velocity distributions, as demonstrated by the results presented in Table I. Notably, all relative errors between the computed average velocities and their corresponding analytical values are less than 2.0%. Hence, it can be inferred that these discrepancies primarily arise from truncation errors inherent in the numerical computations.

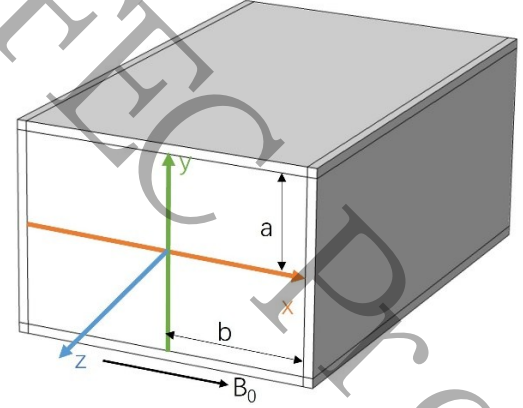


Fig. 1. Schematic of straight rectangular pipe with imposed uniform background magnetic field along x direction.

Table I. Comparison of numerical results with analytical solutions for two Shercliff case and two Hunt cases

Case number	Case 1	Case 2	Case 3	Case 4
Dimensionless parameters	Ha =1000	Ha =1000	Ha =1000	Ha =10000
	$\chi = 1.5$	χ=1.0	χ=1.5	$\chi = 1.0$
	$C_w = 0$	$C_w=0$	$C_{w}=0.016$	$C_{w}=0.05$
Pressure gradient, -dp/dz(Pa/m)	20	20	20	1000
Analytical average velocity, V ₀ (m/s)	4.29×10 ⁻²	1.94×10 ⁻²	0.32×10 ⁻³	1.01×10 ⁻³
Analytical volumetric velocity, Q(m³/s)	2.60×10 ⁻²	7.77×10 ⁻⁴	1.92×10 ⁻⁴	4.05×10 ⁻⁵
Numerical average velocity, V ₀ (m/s)	4.25×10 ⁻²	1.92×10 ⁻²	3.17×10 ⁻³	1.02×10 ⁻³
Numerical volumetric velocity, Q(m³/s)	2.58×10 ⁻²	7.68×10 ⁻⁴	1.98×10 ⁻⁴	4.08×10 ⁻⁵
Relative error in V_0 (%)	0.93	1.03	0.94	1.96

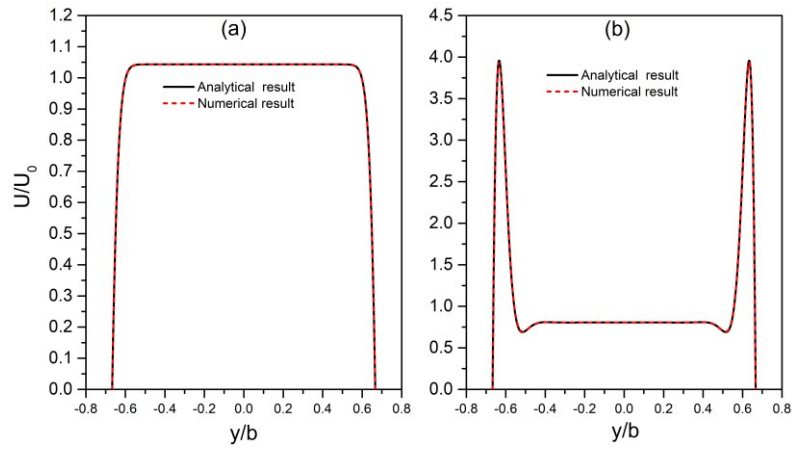


Fig. 2. Comparison of the calculated velocity profiles along the non-dimensional y coordinate with analytical solutions (show in solid line) for case 1 (a) and case 3 (b).

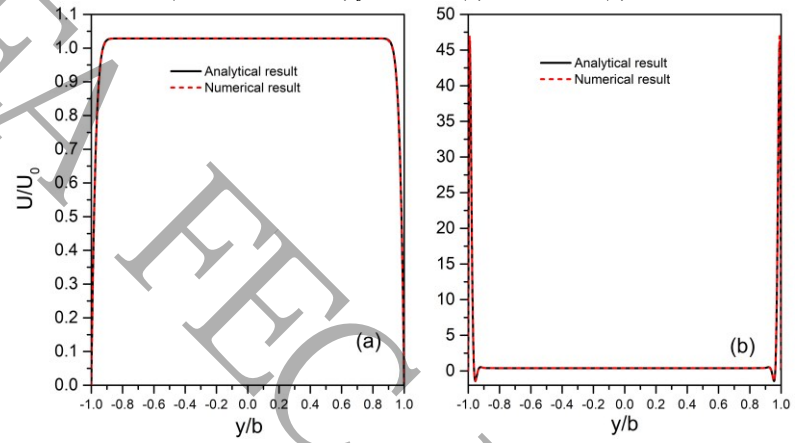


Fig. 3. Comparison of the calculated velocity profiles along the non-dimensional y coordinate with analytical solutions (show in solid line) for case 2 (a) and case 4 (b).

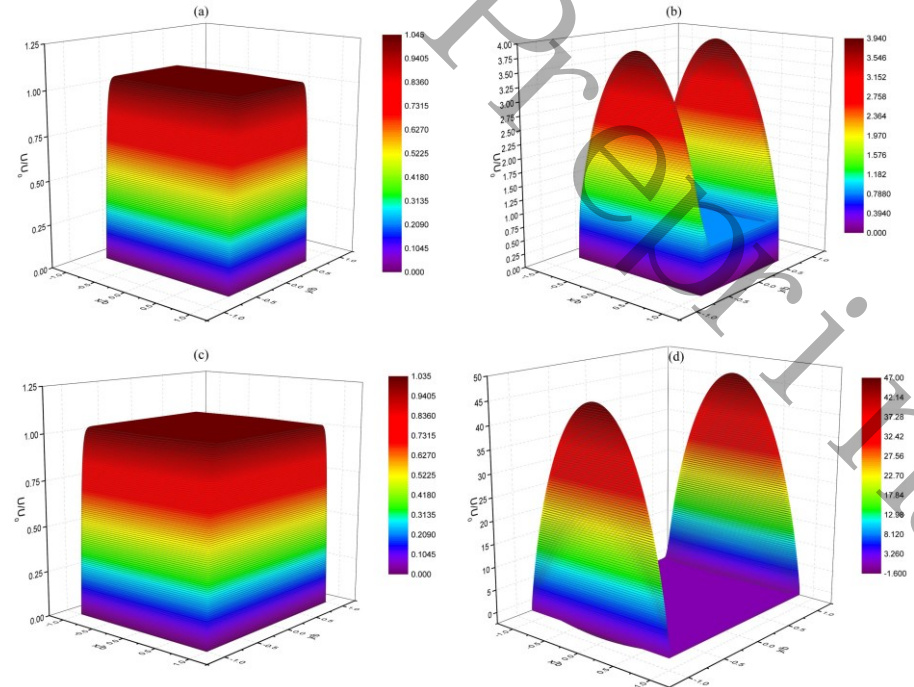


Fig. 4. Fully developed velocity profile on the rectangular pipe cross-section of case 1 (a), case 3 (b), case 2 (c) and case 4 (d).

4. VERIFICATION FOR 3D RECTANGULAR PIPE MHD FLOW CASES IN LONGITUDE VARYING MAGNETIC FIELD

The verification of MHD flow cases in a gradient magnetic field is presented herein. To ensure the reliability of

the MHD code under such conditions, Serge Smolentsev et al. recommend validating the code using the ALEX experiment, which involves studying 3D MHD flow in a rectangular pipe with a non-uniform transverse magnetic field[17]. Here, we carry out numerical simulations to compare with the ALEX experiment data of a square duct MHD flow. In this numerical simulation, the magnetic field is reduced along the flow direction using the data provided by the ALEX experiment. The working fluid is 22Na78k eutectic alloy, and its physical parameters are taken at room temperature. The half-length of the duct cross section is set as 0.048m, and the axial length is 25×0.048m. The flow inlet is set to the fully develop MHD velocity distribution, and its average velocity is 0.34m/s. The pressure at the outlet is set to a constant value. The characteristic parameters of this numerical simulation are consistent with those of the experimental data, Ha=2900 and interaction number, N=540. N is composed of \mathbf{Ha} and Reynolds number, \mathbf{Re} , which is defined as $\mathbf{N} = \frac{\mathbf{Ha}^2}{\mathbf{Re}}$, where \mathbf{Re} is defined as $\mathbf{Re} = \frac{\rho V_0 b}{\mu}$. And the wall thickness and the wall conductivity are adjusted to make C_w =0.07. The pressure gradient along the axial direction obtained by numerical simulation is compared with experimental data in Fig. 5(a). The overall trend of the numerical result is in good agreement with the experimental measurement values, but there is a deviation from the experimental values in the constant magnetic field region. However, it is found that in the region of uniform magnetic field (z<-2), the numerical results are consistent with the pressure drops of the fully developed laminar fluid (Ha=2900, N=540 and $C_w=0.07$) under uniform magnetic field, the constant pressure gradient is 0.052. Therefore, we may speculate that the deviation between the numerical calculation result and the experimental data may come from the error of the experimental measurements. We further perform a comparison of numerically calculated pressure distributions with experimental data. The numerical pressure distribution on the center line of the Hartmann wall and the duct itself and the difference between the above two as well as its corresponding experimental data are shown in Fig. 5 (b). This pressure difference is in good agreement with the overall trend of the experimental measurements, but there is also an observable deviation between the numerical and experimental results at the maximum pressure difference. Narendra Gajbhiya et al. suggest that the data from the ALEX experiment is incomplete and it is challenging to reconstruct a realistic 3D magnetic field based on the available literature. Therefore, they propose using Sterl's case for code validation, which employs thin-wall approximation^[18]. The robust 3D MHD code developed by Narendra Gajbhiya et al. has been validated against ALEX's experiment also and successfully applied to compute sterl's case, yielding results that are in excellent agreement[19][20]. Here, we have adopted Narendra Gajbhiya's validation results with more comprehensive data for validating the 3D MHD code developed in this study. As illustrated in Fig. 6, a vertically acting axially varying magnetic field is applied to a straight rectangular pipe. The computational domain depicted includes a Hartman wall with half-wall length'a', a side wall with half-wall length 'b', and a pipe wall thickness of 0.1 × b. Here, b is equal to a. The wall conductivity ratio is set at $C_w=0.1$, and the fluid volume occupies an area of $8b \times 2a \times 2b$. As demonstrated in the literature [18] and [20], we present a simulation of MHD flow in a rectangular pipe subjected to a transverse nonuniform magnetic field under the conditions of Ha=50, N=1000 and Ha=100, N=1000. The corresponding non-dimensional parameters for these two cases are summarized in Table II. A non-uniform rectangular collocated mesh is employed within the computational domain, incorporating an adequate number of mesh layers in the Hartman layers, sidewall layers, and duct walls to ensure precise numerical calculations. Furthermore, the mesh density is enhanced in regions exhibiting higher magnetic field gradients to accurately capture flow characteristics. The inlet velocity distribution at z/b=0 is assumed to exhibit fully developed ordinary laminar flow. The pressure at the outlet is determined by normalizing the reference value. The non-uniform magnetic field acting on the rectangular flow channel is as follows:

$$B_x = B_0 / \left[1 + e^{-(z/b - 4)/0.15} \right]$$
 (8)

The numerical results were validated for comparison with the Narendra Gajbhiya's results as shown in Fig. 7. In Fig. 7 (a) and (b), the solid lines represent the normalized magnetic field distribution, the dashed lines represent the numerical results in present work, and the signed dashed lines are the results reported by Narendra Gajbhiya^[18]. It should be noted that the figure shows the normalized pressure value. Through the comparison of curve graphics, it is obvious that the numerical results are in good agreement with the reported result. It suggests that the calculations carried out in this work can perfectly reproduce the correct analytical results. At the same time, we also found that the magnetic field gradient has a significant effect on the MHD pressure drops. Although the magnetic field intensity in the variable magnetic field region(3<z/b>
is lower than that in the uniform magnetic field region(5<z/b), the MHD pressure drop gradient in a part of this region is much higher than that in the uniform magnetic field region. This phenomenon appears as a 3D MHD effect caused by magnetic field gradient. The velocity, pressure, and current density distributions on the yz(x/b=0) plane of case 2 are depicted in Fig. 8. It can be observed from Fig. 8 (a) and (c) that at the variable magnetic field region, the dome-shaped fully developed laminar flow at the entrance undergoes a transition to a non-fully developed state under the influence of the

Lorentz force, ultimately evolving into a fully developed laminar MHD flow at downstream with a constant magnetic field. As depicted in Fig. 8 (b), it is evident that the induced current becomes concentrated within the variable magnetic field region, resulting in a heightened local Lorentz force and a more pronounced MHD pressure drops. By analyzing the underlying factors, we posit that within the variable magnetic field region, the lateral fluid movement engenders an additional induced current and consequently generates a greater Lorentz force in this localized area. This phenomenon elucidates why the sidewall layer jet in the variable magnetic field region exhibits more pronounced intensity compared to its counterpart in the constant magnetic field region, as depicted in Fig. 9. The stream-wise velocity profiles at three axial locations viz, z/b=4, z/b=5 and z/b=8 (from top to bottom) for $C_w=0.1$, N=1000 and Ha=50 and Ha=100 are shown in Fig. 9. In particular, the peak value of the side wall layer jets on these three cross sections are the same as Narendra's results. Therefore, the numerical results obtained in this study are total consistent with those reported by Narendra Gajbhiya et al. in terms of pressure distribution and velocity profile. It proved that the code is capable of simulating the whole process of the flow changes from the ordinary laminar flow to the fully developed laminar MHD flow. All in all, the present work has successfully validated the reliability of the developed code in simulating MHD flow cases under non-uniform magnetic fields.

Table II. Dimensionless parameters of Narendra Gajbhiya validation results.

Case numberCase 1Case 2Hartmann number, Ha50100Wall conduction ratio, C_w 0.10.1Interaction Number, N 1×10^3 1×10^3

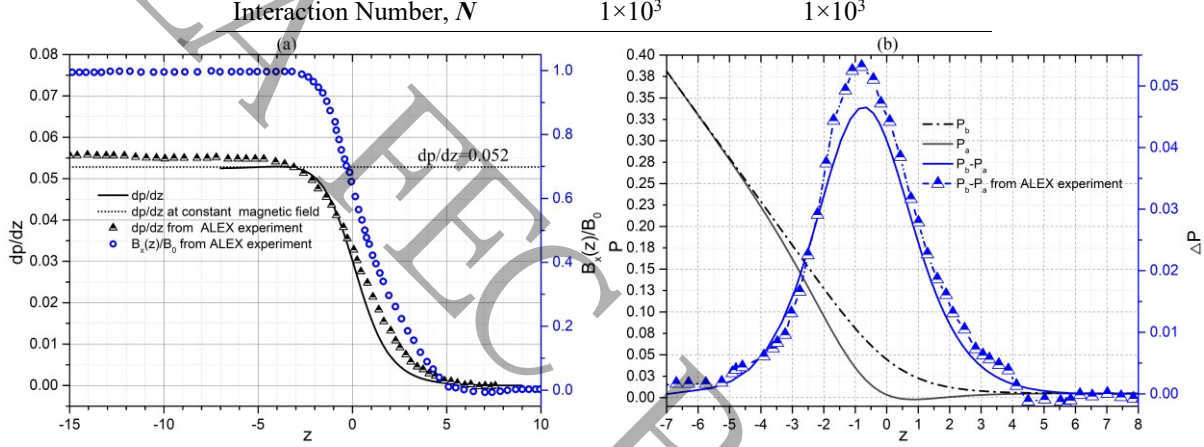


Fig. 5. (a) Comparison between numerical pressure gradient in axial direction and corresponding experiment data, normalized background magnetic field marked with circles, (b) Pressure on the central line of Hartmann wall (P_b) and pressure on the duct central line (P_a) and their difference (P_b - P_a).

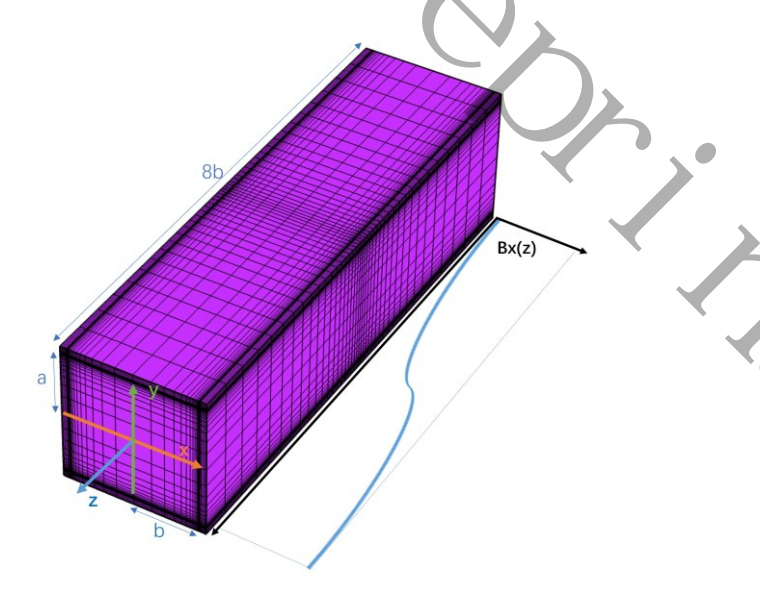


Fig. 6. Schematic of rectangular pipe with imposed non-uniform background magnetic field in x direction.

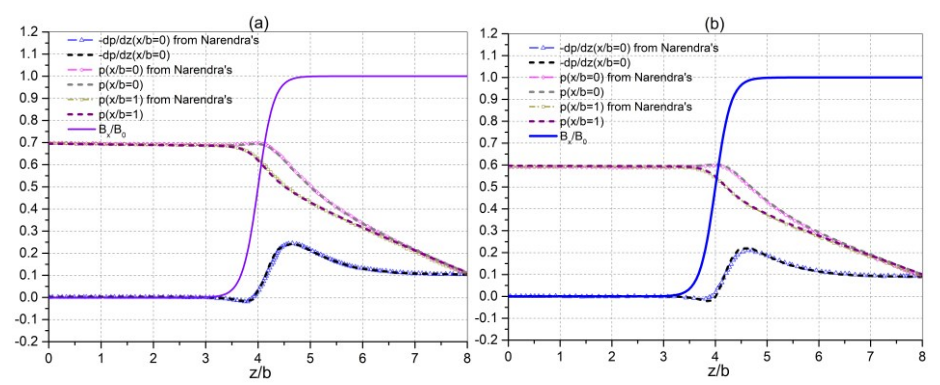


Fig. 7. Comparison of the profiles of the axial(z=0) pressure and pressure gradient in the longitudinal direction obtained in the present work with Narendra for case 1 (a) and case 2 (b).

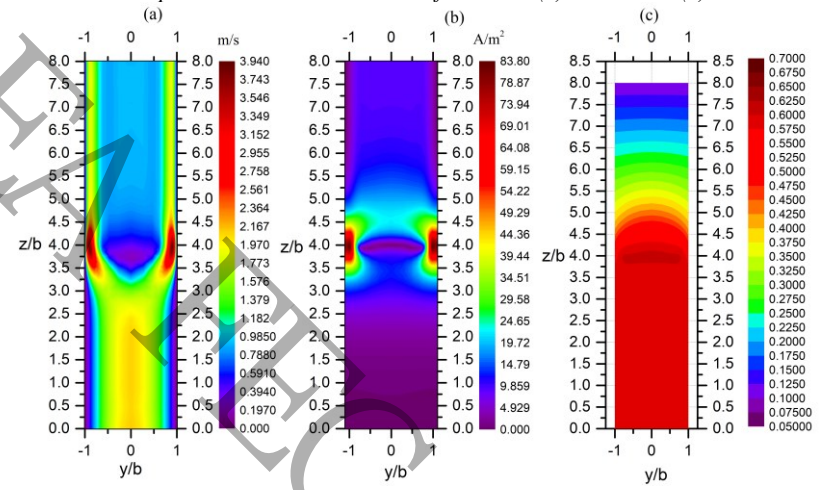


Fig. 8. Normalized velocity distribution (a), current intensity distribution (b) and normalized pressure profile (c) of case 2

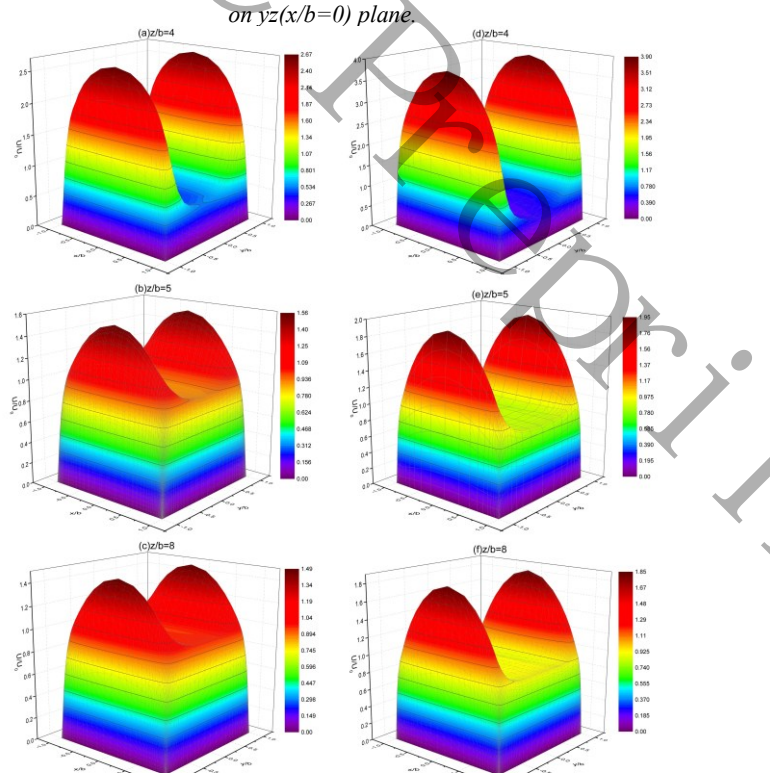


Fig. 9. The velocity profile at three axial locations viz, z/b=4, z/b=5, and z/b=8 (from top to bottom) for Cw=0.1, N=1000 and Ha=50 (left) and Ha=100 (right).

MHD FLOW IN RIPPLED MAGNETIC FIELD

The toroidal magnetic field of a fusion reactor is generated by a finite number of discrete coils arranged toroidally (e.g., the ITER device uses 18 coils). The magnetic field is stronger at the coils and weaker in the gaps between them, and the resulting periodic inhomogeneity is referred to as toroidal field ripple. The region midway between two coils is where the ripple is most significant, with the magnetic field here exhibiting not only a large radial gradient but also a radial component. The inlet and outlet pipes of the liquid lithium-lead blanket typically pass through the mid-region between two coils. Due to the high flow rate of liquid lithium-lead at the inlets and outlets, the pressure drops at these locations constitutes the major portion of the total pressure drop in the blanket. To this end, this study employs a set of toroidally arranged circular coils to simulate the toroidal field of a fusion reactor, aiming to investigate the impact of the rippled magnetic field in the mid-region between two coils on the pressure drops in the inlet and outlet pipes of the liquid lithium-lead blanket. In a fusion reactor, the inlet and outlet pipes of the liquid lithium-lead blanket usually enter and exit vertically through the mid-plane port or upper port to connect with the external loop. Therefore, lithium-lead pipes are arranged at the corresponding positions in the coil model for magnetohydrodynamic analysis. The array of circular coils and the magnetic field they generate are shown in the Fig. 10. The circular coil has a major radius of 3.0 m and a minor radius of 2.5m, with a magnetic field strength of 5 T at the magnetic axis. The inlet rectangular pipe at the upper port is arranged vertically: the plane where the inlet is located is z=1.8 m, the plane where the outlet is located is z=2.8m, and the pipe length is 1 m. The pipe has a Hartmann half-wall length a = 0.1m and a pipe wall thickness of 0.01m. The inlet rectangular pipe at the mid-plane port has the same geometric dimensions as the inlet rectangular pipe at the upper port. For this mid-plane pipe: the plane where the inlet is located is y = 5.8 m, and the plane where the outlet is located is y = 4.8 m. The fluid inside the pipe is liquid lithium-lead, with a dynamic viscosity of 1.93×10^{-3} Pa·s and an electrical conductivity of 7.82×10⁵ S/m. The duct wall is made of reduced-activation steel, whose electrical conductivity is 1.145×10⁶S/m

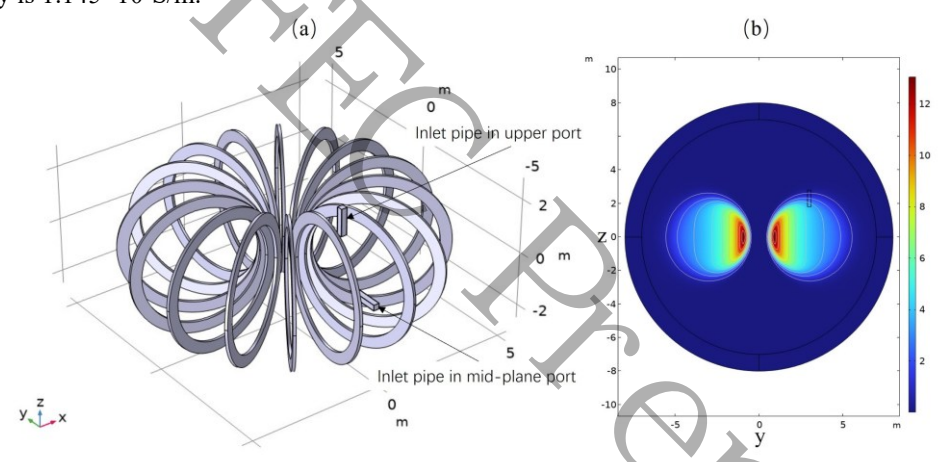


Fig. 10. Toroidally arranged circular coil array for generating a toroidal magnetic field (a) and the distribution of magnetic induction intensity on the YZ plane(b)

The toroidal magnetic field strength decreases rapidly in the region between two coils, and the toroidal magnetic field between the two sets of coils at the upper port, in particular, has a particularly significant gradient. Existing studies have shown that a large magnetic field gradient leads to a three-dimensional MHD pressure drop. However, when the magnetic field varies slowly and the magnetohydrodynamic (MHD) flow remains in a fully developed state, its MHD pressure drop can be characterized by the 2D MHD pressure drop, as shown in Equation (9), wherein C_w is the wall conduction ratio.

$$\Delta P = \int_0^L \frac{c_w}{1 + c_w + 3a/b} U_0 \, \sigma_f [B_0(z)]^2 dz \tag{9}$$
 Here, we compare the numerical calculation results with the fully developed MHD pressure drops calculated by

Here, we compare the numerical calculation results with the fully developed MHD pressure drops calculated by Equation (9) to evaluate the effects of the magnetic field gradient and inhomogeneity of the rippled magnetic field between two coils on the MHD pressure drops and the velocity distribution. The pressure distributions and the applied magnetic field of the liquid lithium-lead MHD flow in the inlet pipes at the mid-plane port and upper port are shown in the Fig. 11. As listed in Table III, the pressure drop values from the numerical calculations are close to those calculated by Equation (9), indicating that the magnetic field gradient and inhomogeneity here can be neglected. In blanket design activities, the pressure drop at the inlet and outlet pipes can be approximately evaluated using Equation (9).

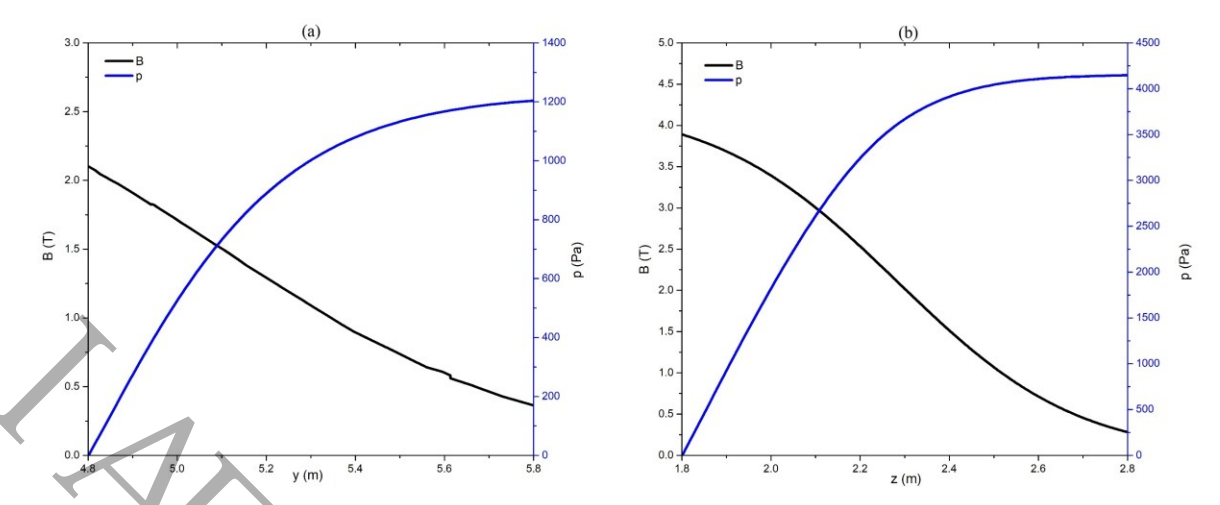


Fig. 11 The pressure distribution along the flow direction and the background magnetic field distribution of the liquid lithium-lead MHD fluid in the rectangular pipes at the mid-plane port (a) and the upper port(b)

Table III. Comparison of numerical calculation results considering the effect of magnetic field gradient with results from 2D fully developed MHD calculations

results from 2D fully developed with calculations					
Case	Inlet MHD flow	Inlet MHD flow			
	in mid-plane	in upper port			
	port				
Pressure drops from numerical	1200 Pa	4147Pa			
calculation considering					
magnetic field gradient					
Pressure drops from2D fully	1246 Pa	4200Pa			
developed MHD calculations					
Discrepancy	3.8%	8.9%			

6. CONCLUSION

A 3D MHD code developed in COMSOL Multiphysics, which solves the magnetic induction formulation and modified Navier-Stokes equations, is employed to simulate incompressible MHD flows under low magnetic Reynolds numbers. This code has been validated against 3D Hunt and Shercliff cases, achieving a maximum Hartmann number of 10,000 in these scenarios. Numerical results show good agreement with literature-reported analytical solutions: the maximum relative error in mean velocities across four validated cases is less than 2.0% (attributed to numerical truncation errors), and transverse velocity profiles closely match analytical predictions. Additionally, the code has been tested on MHD cases with longitudinally varying background magnetic fields, yielding MHD pressure drops, pressure drop gradients, and transverse velocity profiles consistent with literature data. These validations confirm the code's reliability in simulating fully developed laminar MHD flows under uniform magnetic fields, as well as its capability to calculate transitions from ordinary flow to fully developed MHD flow in gradient magnetic fields. Furthermore, the code has enabled investigations into MHD flow behavior under longitudinally varying magnetic fields, facilitating analysis of how magnetic field gradients affect MHD pressure drops and boundary jet flows.

Using this validated code, we investigated the impact of toroidal field ripple—induced by discrete coil arrangements—on pressure drops in the inlet and outlet pipes of liquid lithium-lead blankets, which pass through high-ripple mid-gap regions between coils. Numerical simulations with a toroidal circular coil array analyzed magnetic field distributions at the mid-plane and upper ports, revealing significant toroidal field gradients (particularly pronounced at the upper port). While large magnetic field gradients are known to induce three-dimensional MHD pressure drops, numerical results showed good agreement with the 2D fully developed MHD pressure drop calculations. This indicates that magnetic field gradients and inhomogeneities in the studied regions can be neglected, supporting the reasonable approximation of pressure drops in blanket inlet/outlet pipes using 2D fully developed MHD calculations in design activities.

Future work will focus on enhancing the code's capabilities to better support liquid metal blanket design, including extending it to simulate thermal MHD flows and analyze tritium transport.

ACKNOWLEDGEMENTS

This work was supported by the Innovation Action Program of Southwestern Institute of Physics (No. 202301XWCX005-04).

REFERENCES

- M. A. Abdou, N. B. Morley, S. Smolentsev, A. Ying, S. Malang, A. Rowcliffe, and M. Ulrickson, "Blanket/first wall challenges and required R&D on the pathway to DEMO," Fusion Engineering & Design, 2-43 (2015); https://doi.org/10.1016/j.fusengdes.2015.07.021.
- [2]. U. Muller, L. Buhler, and G. S. Dulikravich, "Magnetofluiddynamics in Channels and Containers," Springer Berlin, 55, 1 (2002).
- [3]. S. Smolentsev, "Physical Background, Computations and Practical Issues of the Magnetohydrodynamic Pressure Drop in a Fusion Liquid Metal Blanket," Fluids, 110 (2021); https://doi.org/10.3390/fluids6030110.
- [4]. S. Smolentsev, N. B. Morley, M. Abdou, and R. Moreau, "Current approaches to modeling MHD flows in the dual coolant lead lithium blanket," Magnetohydrodynamics, 42, 2 (2006).
- [5]. L. Chen, S. J. Xu, M. J. Li, M. J. Ni, and N. M. Zhang, "Study on the impacts of pressure equalization slots on MHD flow and safety of FCI in DCLL blanket," Fusion Engineering & Design, 204-210 (2017); http://dx.doi.org/10.1016/j.fusengdes.2017.08.016.
- [6]. M. J. Ni, R. Munipalli, N. B. Morley, P. Huang, and M. A. Abdou, "A current density conservative scheme for incompressible MHD flows at a low magnetic Reynolds number. Part I: On a rectangular collocated grid system," Journal of Computational Physics, 174–204 (2007); http://dx.doi.org/10.1016/j.jcp.2007.07.025.
- [7]. L. Chen, S. Smolentsey, and M. J. Ni, "Toward full simulations for a liquid metal blanket: MHD flow computations for a PbLi blanket prototype at Ha 10⁴," Nuclear Fusion, 076003 (2020); http://dx.doi.org/10.1088/1741-4326/ab8b30.
- [8]. L. Chen, S. Smolentsev, and M.J. Ni, "Toward full simulations for a liquid metal blanket: part 2. Computations of MHD flows with volumetric heating for a PbLi blanket prototype at Ha 10⁴ and Gr 10¹²," Nuclear Fusion, 026042 (2022); http://dx.doi.org/10.1088/1741-4326/ac3fea.
- [9]. A. Tassone, G. Caruso, A. Del Nevo, and I. Di Piazza, "CFD simulation of the magnetohydrodynamic flow inside the WCLL breeding blanket module," Fusion Engineering & Design, 705–709 (2017); http://dx.doi.org/10.1016/j.fusengdes.2017.05.098.
- [10]. S. Sahu and R. Bhattacharyay, "Validation of COMSOL code for analyzing liquid metal magnetohydrodynamic flow," Fusion Engineering & Design, 151–159 (2018); http://dx.doi.org/10.1016/j.fusengdes.2018. 01.009.
- [11]. C. Alberghi, L. Candido, R. Testoni, M. Utili, and M. Zucchetti, "Verification and Validation of COMSOL Magnetohydrodynamic Models for Liquid Metal Breeding Blankets Technologies," Energies, 5413 (2021); http://dx.doi.org/10.3390/en14175413.
- [12]. M. J. Bluck and M. J. Wolfendale, "An analytical solution to electromagnetically coupled duct flow in MHD," Journal of Fluid Mechanics, 595–623 (2015); http://dx.doi.org/10.1017/jfm.2015.202.
- [13]. C. Kawczynski, S. Smolentsev, and M. A. Abdou, "An induction-based magnetohydrodynamic 3D code for finite magnetic Reynolds number liquid-metal flows in fusion blankets," Fusion Engineering& Design, 422 (2016); https://doi.org/10.1016/j.fusengdes.2016.02.088.
- [14]. J. A. Shercliff, "Steady motion of conducting fluids in pipes under transverse magnetic fields," Mathematical Proceedings, 136–144; http://dx.doi.org/10.1017/s0305004100028139.
- [15]. J. C. R. Hunt, "Magnetohydrodynamic flow in rectangular ducts," Journal of Fluid Mechanics, 577–590; http://dx.doi.org/10.1017/s0022112065000344.
- [16]. S. Smolentsev, N. Morley, and M. A. Abdou, "Code development for analysis of MHD pressure drop reduction in a liquid metal blanket using insulation technique based on a fully developed flow model," Fusion Engineering & Design, 83–93 (2005); http://dx.doi.org/10.1016/j.fusengdes.2005. 01.003.
- [17]. S. Smolentsev, S. Badia, R. Bhattacharyay, L. Bühler, L. Chen, Q. Huang, H. G. Jin, D. Krasnov, D.-W. Lee, E. M. de les valls, C. Mistrangelo, R. Muni- palli, M.-J. Ni, D. Pashkevich, A. Patel, G. Pulugundla, P. Satyamurthy, A. Snegirev, v. Sviridov, P. Swain, T. Zhou, and O. Zikanov, "An approach to verification and validation of MHD codes for fusion applications," Fusion Engineering & Design, 65-72 (2015); http://dx.doi.org/10.1016/j_fusengdes.2014.04.049.
- [18]. N. L. Gajbhiye, P. Throvagunta, and V. Eswaran, "Validation and verification of a robust 3-D MHD code," Fusion Engineering & Design, 7-22 (2018); http://dx.doi.org/10.1016/j.fusengdes.2018.01.017.
- [19]. C. Reed, B. Picologlou, T. Hua, and J. Walker, "ALEX results: A comparison of measurements from a round and a rectangular duct with 3-D code predictions," (1987).
- [20]. A. Sterl, "Numerical simulation of liquid-metal MHD flows in rectangular ducts," Journal of Fluid Mechanics, 161–191 (1990); http://dx.doi.org/ 10.1017/s0022112090000386.